



## Effect of Clamping Pressure and Temperature on the Performance of a CuCl(aq)/HCl(aq) Electrolyzer

Sanchit Khurana,<sup>a,b</sup> Derek M. Hall,<sup>a,b</sup> Rich S. Schatz,<sup>a,b</sup> and Serguei N. Lvov<sup>a,b,c,\*</sup>,<sup>z</sup>

<sup>a</sup>Department of Energy and Mineral Engineering, The Pennsylvania State University, University Park, Pennsylvania 16802, USA

<sup>b</sup>The EMS Energy Institute, The Pennsylvania State University, University Park, Pennsylvania 16802, USA

<sup>c</sup>Department of Materials Science and Engineering, The Pennsylvania State University, University Park, Pennsylvania 16802, USA

Changes in the performance of a CuCl(aq)/HCl(aq) electrolytic cell are reported as a function of temperature and the compression pressure applied at the end plates during cell assembly. The pressure applied on the end plates effected the contact resistance, and an optimum compression pressure of 6.3 psi (bolt torque: 20 Nm) showed the best performance. Polarization curves and EIS data were taken at 40, 60, and 80°C to observe the changes in ohmic and nonohmic impedance contributions. A significant increase in the cell performance was observed as the temperature was increased from 40 to 80°C.

© The Author(s) 2015. Published by ECS. This is an open access article distributed under the terms of the Creative Commons Attribution 4.0 License (CC BY, <http://creativecommons.org/licenses/by/4.0/>), which permits unrestricted reuse of the work in any medium, provided the original work is properly cited. [DOI: 10.1149/2.0011504eel] All rights reserved.

Manuscript submitted December 2, 2014; revised manuscript received January 15, 2015. Published February 5, 2015.

The Cu-Cl thermochemical cycle is among the most attractive technologies proposed for hydrogen production,<sup>1-4</sup> and significant improvements in the current and voltage efficiencies of the CuCl(aq)/HCl(aq) electrolytic cell – a key component in the cycle – have recently been reported.<sup>5-7</sup> In our previous work,<sup>7</sup> kinetic properties of the CuCl electrolyzer were investigated to successfully reduce the catalyst loading by 68% without causing any adverse effect on the cell performance and durability of the cell was reported for 168 h of operation.<sup>8</sup>

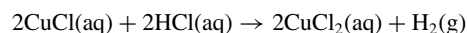
A significance performance limitation for a CuCl(aq)/HCl(aq) electrolytic cell is the ohmic losses associated with the contact resistance. The contact resistance between the flow field channels of the end plate and the carbon cloth electrodes plays a significant part in ensuring good electrical connection. The contact resistance is heavily dependent on the clamping pressure, and despite the link between compression and electrochemical performance, there are no published results related to optimum amount of pressure needed to assemble a CuCl(aq)/HCl(aq) electrolytic cell. While insufficient clamping pressure may result in high electrical resistance at the electrodes/flow-field channel interface, a high clamping pressure could lead to mechanical deformation of the MEA and uneven pressure distribution. An excessive compression pressure also increases the mass transport problems with a reduction in cell performance at high current densities.<sup>9,10</sup> In this study, an optimum value of the compression pressure resulting from torque on the bolts that clamp the cell was observed to be 20 Nm. Also, this study highlights the increase in performance of a CuCl(aq)/HCl(aq) electrolyzer by increasing the temperature from 40 to 80°C.

### Experimental

**Preparation of MEA.**— The experimental setup consisting of Nafion 117 polymer membrane, which was used to fabricate the MEA, and the pretreatment method was same as discussed previously.<sup>6</sup> The membrane was pretreated by the following steps to remove the organic and inorganic contaminants before being used in the electrolyzer. First, the membrane was soaked in 3 wt% H<sub>2</sub>O<sub>2</sub> solution at 80°C, followed by soaking in 80°C DI-water to remove traces of H<sub>2</sub>O<sub>2</sub>. Then, the membrane was soaked in 1 mol L<sup>-1</sup> H<sub>2</sub>SO<sub>4</sub>(aq). Finally, the membrane was soaked in DI-water at 80°C to remove any residual H<sub>2</sub>SO<sub>4</sub>(aq). The membrane was placed in each solution for 1 h. The membrane was dried overnight in a desiccator and hot-pressed at

93.33°C before being allowed to cool at the room temperature. Two 5 cm<sup>2</sup> carbon-cloth electrodes (GDL 10 AA, Ion Power Inc), brush painted with 4 mg cm<sup>-2</sup> of XC-72 R catalyst with 20% Pt (0.8 mg cm<sup>-2</sup> Pt), were placed on each side of the membrane before installing in the electrolyzer. The catalyst ink was prepared by mixing 15% Nafion EW 1100 solution with 20% platinum on Vulcan XC-72R in a ratio of 2.86:1 Nafion to Vulcan XC-72R by weight.<sup>7</sup>

**Operation and stability of a single cell.**— The CuCl electrolysis can be represented by the following reaction:



However, it should be noted that the anodic reaction, which involves the oxidation of Cu(I) to Cu(II), consists of a number of intermediate species discussed elsewhere.<sup>11</sup>

Two 85 cm<sup>2</sup> graphite blocks having serpentine flow channels were obtained from Electrochem Inc. and used as the end plates. 2 mol CuCl(s) dissolved in 7 mol L<sup>-1</sup> HCl (aq), and 7 mol L<sup>-1</sup> HCl(aq), were, respectively, fed into the anode and the cathode electrodes with a flow rate of 130 ml min<sup>-1</sup>. Variable values of clamping torques –5, 10 and 20 Nm – were applied on the end plate bolts, which correspond to 1.7, 3.2, and 6.3 psi pressure values, respectively. The objective was to ensure good electrical contact between the loose components of the MEA. After setting a baseline for the ohmic resistance, a separate experiment was performed to observe the changes in performance of the cell by increasing the temperature from 40 to 80°C.

**Electrochemical techniques.**— Electrochemical measurements were made using Gamry Reference 3000 potentiostat. For EIS measurements, 10 mV of voltage perturbation was applied by sweeping the frequency from 0.01 Hz–50 kHz with 10 points per decade interval. The data were obtained at OCP and at an applied potential of 0.4 V. A delay of 2 minutes was applied between each measurement in order to allow the cell reaching the steady-state. Consistency and quality of data were established by Kramers-Kronig validation.<sup>12</sup>

Polarization curves were taken with a scan rate of 10 mV s<sup>-1</sup> to obtain the current density values for the 0–0.7 V (applied potential) range. Polarization curves were obtained before and after EIS measurements to ensure that the cell characteristics were not changed.

### Results and Discussion

Figure 1 represents the impedance plots at different compression values and corresponding polarization curves reflecting an increase in the current density are shown in Figure 2. Since all other major factors effecting the bulk resistance of the cell components were kept

\*Electrochemical Society Active Member.

<sup>z</sup>E-mail: lvov@psu.edu

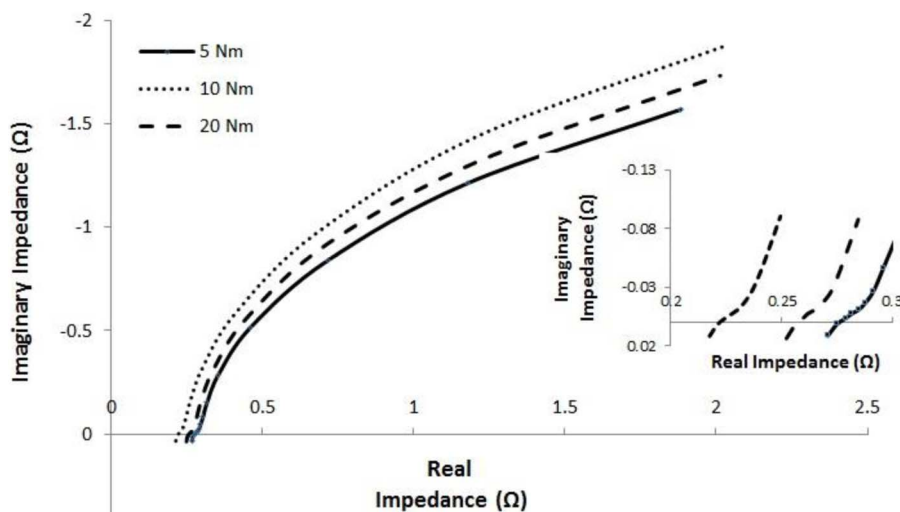


**Figure 1.** Decrease in ohmic resistance as the clamping torque was increased from 5 to 20 Nm by altering the applied pressure from 1.7 psi to 6.3 psi. The inset shows the high frequency intercept corresponding to the ohmic resistance of the cell. The data were taken at 30°C.

constant (anode and cathode solutions flow rate, temperature etc.), it is safe to assume that the variations in ohmic resistance are primarily dependent on the contact resistance of the cell. A gradual decrease in the ohmic resistance of the cell from 0.27 to 0.21  $\Omega$  was observed as the clamping torque was increased from 5 to 20 Nm by applying pressure from 1.7 psi to 6.3 psi. Therefore, 20 Nm was selected as the optimum bolt torque to minimize the contact resistance. It should also be noted that any excessive pressure beyond this point may result in increased mass transfer resistance which prevails at high clamping torques.

As shown in Figure 3, the electrochemical performance of the cell increased with the increase in temperature. The current densities at an applied potential of 0.7 V at 40 and 80°C were observed to be 0.27 and 0.40  $\text{A cm}^{-2}$ , respectively. In order to account for this 48% increase in performance, EIS data were taken in a separate experiment at room temperature (30°C) and 80°C at an applied potential of 0.4 V. Figure 4 shows a large decrease in overall impedance of the cell as the temperature was increased. The EIS data gives insight about the changes in ohmic resistance ( $R_s$ ), and two faradaic impedances observed as two distinct arcs ( $R_1$  and  $R_2$ ) in the Nyquist plot. The equivalent circuit model shown as the inset in Figure 4 was used to simulate the experimental data. The fit converged satisfactorily, and the chi-squared ( $\chi^2$ ) parameter, representing the goodness of fit was  $3 \times 10^{-5}$ . The high-frequency inductance was believed to be an instrumental artifact and corrected with  $2.45 \times 10^{-6}$  H. It was found that the ohmic resistance of the cell decreased from 0.21 to 0.13  $\Omega$  as the

temperature was increased from 30 to 80°C. As the membrane resistance is almost equal to the ohmic resistance of the cell,<sup>8</sup> the decrease in ohmic resistance is primarily attributed to the increase in membrane conductivity with an increase in temperature.<sup>13</sup> The nonohmic impedance contribution decreased from 4.8 to 0.27  $\Omega$ . While it is difficult to correctly interpret the faradaic impedances as the cell reaction mechanism has not been well-established yet,<sup>11</sup> we have previously shown<sup>8</sup> that  $R_1$  is dependent on the applied potential and related to the charge-transfer kinetics. As the anodic reaction in the cell is significantly faster than the cathode,<sup>7</sup> it is fair to assume that the anode kinetics are faster at 80°C. The charge-transfer kinetics, along with a significant decrease in the ohmic resistance at 80°C, result in a 48% increase in the current density at an applied potential of 0.7 V.

## Conclusions

The contact resistance between the flow field channels of the end plate and the carbon cloth electrodes interface was heavily dependent on clamping torque and an optimum compression pressure of 6.3 psi (bolt torque: 20 Nm) was selected based on the ohmic resistance measurements. The CuCl electrolyzer was operated at different temperatures, and LSV along with EIS were successfully applied to monitor the system behavior with changes in temperature. A 48% increase in the current density was observed at an applied potential of 0.7 V as the temperature was raised from 40 to 80°C. An equivalent circuit model was used to quantify the changes in ohmic and nonohmic impedance contribution at different temperatures. For the Cu-Cl thermochemical cycle to be commercially viable,

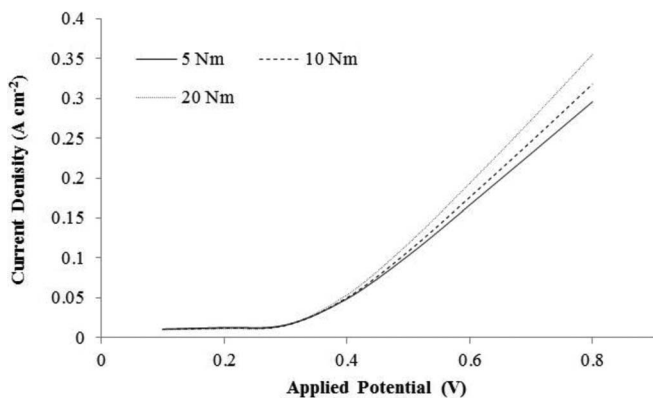


**Figure 2.** Polarization curves representing increase in the overall performance as the clamping torque was increased by altering the applied pressure. The data were taken at 30°C.

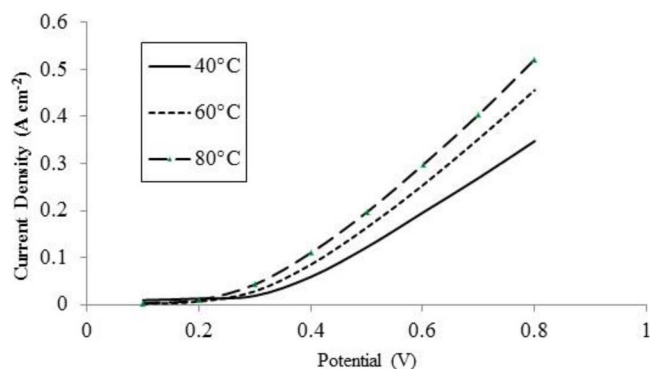


**Figure 3.** Polarization curves showing the increase in the current density as the temperature was raised from 40 to 80°C.

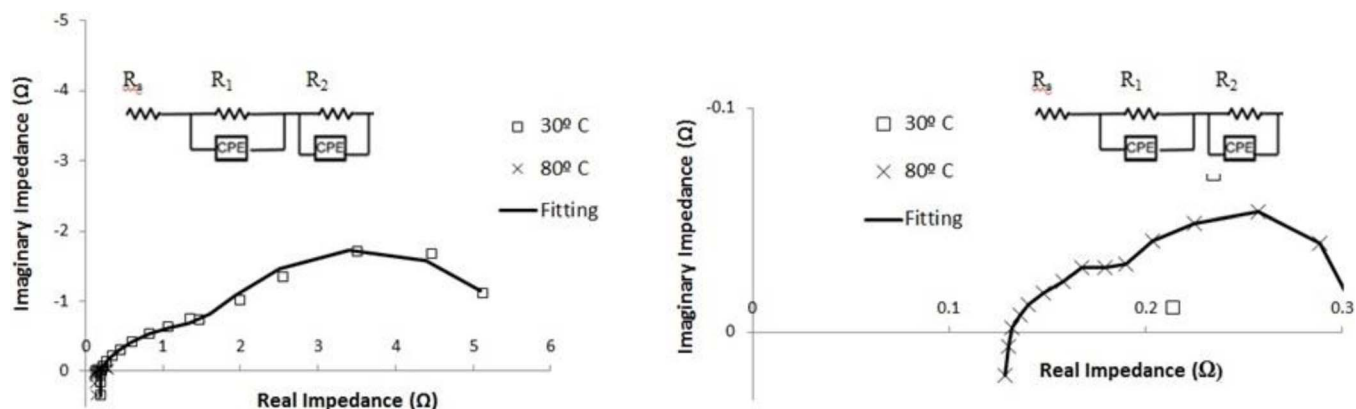


**Figure 4.** EIS data at 30 and 80°C along with the circuit model for the cell operating at an applied potential of 0.4 V (left) and the zoomed in section (right) to highlight the impedance data at 80°C. The inset represents the equivalent circuit model used to fit the experimental data.

electrolysis is a key step and this study provides pathways to substantially improve the performance by selecting optimum assembly and operating conditions.

### Acknowledgments

The authors gratefully acknowledge the financial support of this work by U.S. Department of Energy's Office of Energy Efficiency and Renewable Energy via a subcontract with Argonne National Laboratory. We thank Dr. Mark Fedkin, Michele Lewis and Shabbir Ahmed for their useful feedbacks on the obtained data.

### References

1. G. Naterer, S. Suppiah, M. Lewis, K. Gabriel, I. Dincer, M. A. Rosen, M. Fowler, G. Rizvi, E. Easton, and B. Ikeda, *Int J Hydrogen Energy*, **34**, 2901 (2009).
2. G. Naterer, S. Suppiah, L. Stolberg, M. Lewis, M. Ferrandon, Z. Wang, I. Dincer, K. Gabriel, M. Rosen, and E. Secnik, *Int J Hydrogen Energy*, **36**, 15472 (2011).
3. M. S. Ferrandon, M. A. Lewis, D. F. Tatterson, R. Nankanic, M. Kumarc, L. E. Wedgewood, and L. C. Nitsche, in: *NHA annual hydrogen conference, Sacramento convention center, CA, 2008*, pp. 3310–3326.
4. G. Naterer, S. Suppiah, L. Stolberg, M. Lewis, S. Ahmed, Z. Wang, M. Rosen, I. Dincer, K. Gabriel, and E. Secnik, *Int J Hydrogen Energy*, **39**, 2431 (2014).
5. V. N. Balashov, R. S. Schatz, E. Chalkova, N. N. Akinfiev, M. V. Fedkin, and S. N. Lvov, *Journal of the Electrochemical Society*, **158**, B266 (2011).
6. R. Schatz, S. Kim, S. Khurana, M. Fedkin, and S. N. Lvov, *ECS Transactions*, **50**, 153 (2013).
7. D. M. Hall, E. G. LaRow, R. S. Schatz, J. R. Beck, and S. N. Lvov, *Journal of The Electrochemical Society*, **162**, F108 (2015).
8. S. Khurana, D. M. Hall, R. S. Schatz, M. V. Fedkin, and S. N. Lvov, *Int J Hydrogen Energy*, **40**, 62 (2015).
9. C.-Y. Wen, Y.-S. Lin, and C.-H. Lu, *Journal of Power Sources*, **192**, 475 (2009).
10. P.-H. Chi, S. Chan, F. Weng, A. Su, P. Sui, and N. Djilali, *Int J Hydrogen Energy*, **35**, 2936 (2010).
11. D. M. Hall, N. N. Akinfiev, E. G. LaRow, R. S. Schatz, and S. N. Lvov, *Electrochimica Acta*, **143**, 70 (2014).
12. M. C. Lefebvre, R. B. Martin, and P. G. Pickup, *Electrochemical and solid-state letters*, **2**, 259 (1999).
13. Y. Sone, P. Ekdunge, and D. Simonsson, *Journal of the Electrochemical Society*, **143**, 1254 (1996).